Original Article

# Effect of Celastrol and Celastrol Nanoemulsions on Regeneration of Mandibular Bone Defects in Osteoporotic Rats

***Laila F. Elshahed[1], Doaa A. Labah[1], Rasha M. Taha[2], Tamer H. Hassan[3] and Elham F. Mahmoud[2]***

*Department of Oral Biology, Faculty of Dentistry, [1]Zagazig University, [2]Suez Canal University, Egypt*

*[3]Department of Pharmaceutics and Industrial Pharmacy, Faculty of Pharmacy, Suez Canal University, Egypt*

## ABSTRACT

**Introduction:** Osteoporosis is a skeletal-metabolic disease characterized by low bone mineral density and deterioration of bone microarchitecture. Poor bone quality due to osteoporosis complicates the healing process. Thus, developing new strategies for prevention and treatment of osteoporosis represent an urgent need. Chinese herbal medicines are gaining attractiveness in traditional medicine.

**Aim to the Work:** To detect and compare the effect of celastrol (CTL) and Celastrol nanoemulsions (CTL-NE) on the regeneration of mandibular bone defects in ovariectomized (OVX) rats as a model of postmenopausal osteoporosis (PMOP).

**Material and Methods:** Sixty female rats were randomly distributed into two groups: sham group and OVX group. Sixty days following OVX and sham operations, a bone defect in the mandible was created in all rats. Then, the rats of each group were further subdivided equally into 3 subgroups; subgroup1: the rats were left without any treatment, subgroup 2: the animals received a daily dose of CTL for 4 weeks and subgroup 3: the rats received a daily dose of CTL-NE for 4 weeks. At the end of the experiment, the rats were euthanized and their lower jaws were prepared for examination qualitatively by histological, scanning electron microscope (SEM) examination and quantitatively by X-ray microanalysis.

**Results:** Histological and ultrastructural examination showed that osteoporotic rats had compromised bone regeneration with many signs of delayed bone defect healing. Besides, elemental microanalysis of the osteoporotic defect exhibited significant reduction in its calcium content. Interestingly both sham and OVX groups obtained better defect healing upon CTL administration, however, superior healing was achieved in CTL-NE treated rats. These results were confirmed histologically, ultrastructurally and qualitatively by calcium elemental microanalysis.

**Conclusion:** Systemic administration of CTL and CTL-NE may be an effective therapy for treatment of osteoporotic bone defects, with privilege to CTL-NE therapy in terms of quantity and quality of regenerated bone.

**Received:** 10 January 2025, **Accepted:** 30 January 2025

**Key Words:** Bone healing, celastrol, nanoemulsions, osteoporosis.

**Corresponding Author:** Laila Fikry Elshahed, PhD, Department of Oral Biology, Faculty of Dentistry, Zagazig University, Zagazig, Egypt, **Tel.**: +20 10 1554 0999, **E-mail:** lfelsayed@dent.zu.edu.eg

**ISSN:** 1110-0559, Vol. 48, No. 2

## INTRODUCTION

Osteoporosis is a skeletal-metabolic disease characterized by a decline in bone mineral density and disturbance of the bone microarchitecture. About 200 million people worldwide suffer from osteoporosis, including 34% of women over 50 and it is termed postmenopausal osteoporosis “PMOP”, which is caused mainly by estrogen deficiency[1].

The clinical consequences of this systemic disorder mainly include an increased risk of bone fractures. Poor bone quality associated with PMOP seriously complicates the healing process. There is an urgent need to develop novel strategies for prevention and treatment of osteoporosis-induced fractures which is the most serious complication of PMOP as they are linked to increased morbidity and death as well as a significant economic burden[2].

Numerous medications for treating osteoporosis have been studied and they are available in the market. Osteoporosis can be effectively treated and prevented with traditional anti-osteoporotic medications. But because of their numerous negative effects, many women turn to herbal preparations as an alternative form of treatment. Traditional herbal medicine has recently drawn more attention since it contains a many bioactive components that are awaiting discovery and research[3].

The "thunder god vine" is the common name for Tripterygium wilfordii. In China, it has long been used to treat autoimmune conditions such type 1 diabetes, Crohn's disease, and rheumatoid arthritis. Triterpenoids and alkaloids, which are mostly taken from the plant's root pulp, are among the phytochemicals that are abundant in the plant. Celastrol (CTL) is the most prevalent and promising bioactive molecule among these phytochemicals[4].

*DOI: 10.21608/ejh.2025.347054.2186*

Over the past 20 years, CTL, also referred to as tripterine, has become more significant because of its strong anti-inflammatory, anti-cancer, neuroprotective, and antioxidant properties. Nevertheless, despite its potency, its clinical translation is hindered by two primary drawbacks: its narrow therapeutic index, which results in substantial systemic toxicity, and its poor water solubility, which restricts its bioavailability at 25°C (0.044 mg/ml)[5].

Numerous medication delivery strategies have been studied in an effort to address the toxicity concerns while maintaining the intended therapeutic efficacy. Because of its smaller size, targeting potential, and improved solubility and permeability—two factors that are beneficial in boosting the bioavailability of CTL—nanoparticulate drug delivery systems and nanoformulations of CTL have been highlighted as a promising approach[6].

Nanoemulsions are one type of nanotechnology. Fine oil-in-water dispersions with droplets ranging in size from 100 to 600 nm make up nanoemulsions. It was demonstrated that CTL-NE might enhance CTL's oral bioavailability, therapeutic benefits, and tissue targeting capacity[7].

## MATERIALS AND METHODS

### *Animals*

The current study was an experimental investigation carried out with permission from the Suez Canal University Faculty of Dentistry's Research Ethics Committee (REC), bearing approval number (403/2021).

The sample size was determined[8] with 30 samples each group and 10 samples per subgroup, the anticipated sample size was 60 samples total (n=60).

For this investigation, 60 female Sprague-Dawley rats weighing between 250 and 300 g and 6 months of age were acquired from Zagazig University's Faculty of Medicine. The rats were kept in suitable circumstances in cages and given water and soft food. Rats were randomly assigned into two major groups of thirty after a week of acclimation to the new laboratory conditions: an OVX group and a sham group.

### *Construction of the osteoporosis model*

Ketamine-Xylazine (K: 75–90 mg/kg + X: 5–10 mg/kg in the same syringe) was injected intraperitoneally to anesthetize the animals before the surgery. Bilateral ovarian excision was carried out in the OVX group using the dorsal technique, as previously reported by[9]. Similar surgery was performed on the sham group, exposing the ovaries and reinstalling them in the same location without removing them. The El-Borg laboratory's Zagazig branch's examination of the serum estradiol level (E2) verified the ovariectomy's effectiveness (Figure 1).

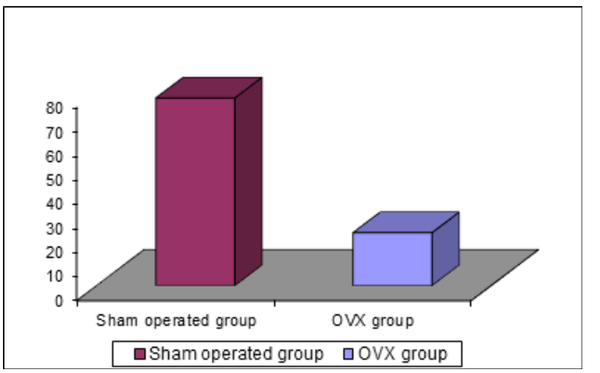


**Fig. 1:** Histogram shows the mean estradiol levels in both sham and OVX groups.

### *Establishment of mandibular defect model*

sixty days after the ovarian excision was confirmed to be successful and after OVX and sham procedures (Figure 1). Ketamine-Xylazine (K: 75–90 mg/kg + X: 5–10 mg/kg in the same syringe) was injected intraperitoneally to anesthetize the experimental rats. A slow-speed dental drill (Dentsply sirona, US) was used to create 5x5 mm full thickness critical defects in the right side of the mandible's body (near the angle of the mandible) while maintaining continuous normal saline irrigation to avoid overheating. Following the creation of the defect, the area was heavily irrigated with regular saline to get rid of any remaining bone pieces. Using 4-0 Vicryl suture (Ethicon, Lenneke Marelaan, Belgium), the soft tissues above the defect were sutured in layers. Penicillin (Pipeline Pharma, Vilnius, Lithuania) at 40,000 IU/ml, 1 ml/kg, was administered intramuscularly for three days following surgery[10].

### *Preparation of the CTL-NE*

CTL-NE preconcentrate was prepared by mixing 200 mg of CTL extract (Sigma-Aldrich, MO, USA) with purity greater than 98% with a mixture of 40% Capryol 90 (Gattefosse, Saint-Priest, France) and 60% Tween 80 (ADWIC Chemicals Co. Cairo, Egypt). The preconcentrate was diluted with purified water to generate nanoemulsions prior to the experiments.

### *Characterization of CTL-NE*

#### Transmission Electron Microscopy (TEM)

Transmission electron microscopy (TEM, JEOL JEM-2010, Japan) linked to a Gatan camera at Faculty of Agriculture, Mansoura University, and operating at a 200 kV accelerating voltage was used to measure the size and shape of the produced CTL-ND.

#### Zeta Potential measurement

Using a Zetasizer Nano ZS (Malvern Instruments Ltd., Malvern, UK), the zeta potential (ZP) was measured precisely at 25°C. Three duplicates of each measurement were made, and the mean ± standard deviation (SD) was used to describe the results. A suitable volume of distilled water was used to dilute each sample 20 times before analysis.

### *Animal subgrouping and drug administration*

The rats of each group were further sectioned into 3 subgroups of 10 rats, the sham group was sectioned into: a) Subgroup 1.1 where the rats were left without any treatment, b) Subgroup 1.2 in which the animals received a daily dose of CTL (1.5mg/kg/day) orally by gavage for 4 weeks, c) Subgroup 1.3 where the rats were given a daily dose of CTL-NE (1.5mg/kg/day) orally by gavage for 4 weeks. While the OVX group was subdivided into: a) subgroup 2.1 in which the rats didn't had any treatment, b) subgroup 2.2 where the rats received a daily dose of CTL (1.5mg/kg/day) orally by gavage for 4 weeks similar to subgroup 1.2 and finally c) subgroup 2.3 where the rats were given a daily dose of CTL-NE (1.5mg/kg/day) orally by gavage for 4 weeks similar to subgroup 1.3[11].

### *Euthanasia and sample collections*

Rats were euthanized after finishing the treatment protocol for each group (4 weeks after the mandibular bone defect surgery) by overdose inhalation of Ether (Sigma-Aldrich, MO, USA)[12]. The lower jaw of each rat was dissected out, and their right halves were collected and immediately fixed with buffered formalin solution. Five specimens per group were prepared for histological examination and five other samples per group were prepared for X-ray elemental microanalysis and SEM examination.

### *Histological evaluation*

After fixation, the specimens were decalcified in 5% formic acid. After complete decalcification, specimens were washed in distilled water, dehydrated in ascending grades of ethyl alcohol, cleared in xylene and embedded in paraffin. Serial sections (5µm) were cut and stained with hematoxylin and eosin (H&E)[13]. Afterward, the slides were visualized in a light microscope equipped with a built-in camera (OPTIKA Digital binocular brightfield microscope) at Histology department, Faculty of Medicine, Zagazig University.

### *X-ray elemental microanalysis*

After fixation, the samples treated with 5% sodium hypochlorite (commercial bleach), for 1 hour, to eliminate the organic material. After distilled water washing, specimens were dehydrated in ethanol, air-dried and examined by energy dispersive x-ray analysis (EDAX) attached with the SEM. This technique is designed to analyze the inorganic constituents (mainly calcium level) of the specimens.

### *SEM evaluation*

After detection of their elemental composition, the samples were ready for SEM examinations. They were vacuumed, covered with gold through Blazers' SCD-050 sputter that converted electrically non-conductive samples into conductive ones hence enabled a tightly focused electron beam to be scanned across the sample surface by SEM (JEOL JSM-636 OLA, Japan, at an accelerating voltage of 15kv) at EM unit, Mansoura University, Egypt.

### *Statistical Analysis*

One-way ANOVA (analysis of variance) was used to conduct statistical analyses of the calcium levels. The statistical significance between the subgroups was assessed using Tukey's post hoc test. A *P value* of less than 0.05 is regarded as statistically significant. Version 22.0 of the SPSS software for Windows (Statistical Package for Social Science, Armonk, NY: IBM Corp.) was used to conduct the analysis.

## RESULTS

### *Osteoporosis induction*

The induction of osteoporosis was confirmed by analysis of serum E2 level. Rats of the sham group showed mean E2 of 77.57 U/L. while OVX rats displayed mean E2 of 21.86 U/L (Figure 1)

### *Preparation of the CTL-NE*

Based on preliminary CTL solubility study, both Capryol 90 and Tween 80 were selected as CTL-NE excipient. CTL-NE was prepared as a water-free self-nanoemulsifying preconcentrate to enhance shelf-life stability.

### *Characterization of the CTL-NE*

#### Morphological analysis

Morphological analysis revealed homogenous spherical shaped particles. The size of developed dispersions was around 460 nm. Moreover, they were separated from each other without aggregation indicating effectiveness (Figure 2 A).

#### The zeta potential analysis (ZP)

The zeta potential detected for the synthesized CTL-NE was -60 mV. This highly negative zeta potential value reflects that the nanoemulsions possess high stability (Figure 2 B).

### *Histological evaluation*

In the sham group, the defect in subgroup 1.1 was incompletely closed with newly formed bones in which the osteocytes exhibited large size and irregular arrangement while the rest of the defect was still filled with granulation tissue (Figure 3 A). In subgroup 1.2, there was a noticeable decrease in the defect size compared with subgroup 1.1. However, a part of the defect was also filled with a small amount of granulation tissue (Figure 3 B). Whereas the bone defect in subgroup 1.3 was almost closed with newly formed bone in which few marrow spaces were scattered (Figure 3 C).

In OVX group, delayed bone healing could be noticed in subgroup 2.1 as the defect site was almost filled with granulation tissue in which numerous fat vacuoles and multinucleated giant cells were scattered (Figure 3 D).

Subgroup 2.2 showed improvement regarding bone healing, although the defect was incompletely closed and a part of it was still occupied by granulation tissue (Figure 3 E). In subgroup 2.3, the defect site appeared almost completely healed with new bone trabeculae. However, few marrow spaces were still evident. Also, multiple dense resting lines were notable within the newly formed bone (Figure 3 F).

### *X-Ray Elemental Microanalysis*

Representative spectra of the mandibular bone defect areas of the different subgroups revealed variations in their elemental composition. The changes in the relative calcium (Ca) levels between them were considerable. Statistical analysis demonstrated that subgroup 1.3 recorded the highest mean value for Ca level while subgroup 2.1had the lowest value for Ca level. In sham group, subgroup 1.2 had significantly lower Ca level than subgroup 1.3 and higher levels than those of subgroup 1.1. While in OVX subgroups, Ca level in subgroup 2.2 was verified to be significantly higher than subgroup 2.1 and significantly lower than subgroup 2.3. In addition, subgroup 2.1 and subgroup 2.2 had significantly lower Ca values than those of all the sham subgroups. Also, the mean Ca value of subgroup 2.3 revealed significant increase than that of subgroup 1.1 (Figure 4).

### *Scanning electron microscopy*

In sham group, SEM examination of the defect area in subgroup 1.1showed that it was healed with newly formed bone with its characteristic unordered bone trabeculae and numerous marrow spaces of variable shape and size. Furthermore, the lacunae of osteocytes were roundish, large in size and randomly distributed among the newly formed trabeculae (Figure 5 A). In subgroup 1.2, the healing callus was composed of newly created bone trabeculae in the middle of the defect, encircled by callus lamellar bone with elliptical osteocyte lacunae. It is impossible to differentiate this callus lamellar bone from the original lamellar compact bone since they have fused together (Figure 3 B). The defect in subgroup 1.3 was almost completely restored with callus lamellar bone. This callus lamellar bone had more dense coalesced bone compared with the disorganized preexisting woven bone and less compacted bone structure compared with the original cortical bone (Figure 5 C).

In OVX group, delayed bone healing could be noticed in subgroup 2.1 where the center of the defect appeared hollow and devoid of any healing callus except of a small bony callus. Also, little new thin bone trabeculae were detected at some parts of the cavity margin, however it couldn't be detected at others (Figure 5 D). In subgroup 2.2, the defect was incompletely healed by newly formed bone composed of poorly arranged bone trabeculae separated from each other by marrow spaces of variable shape and size (Figure 5 E). While in subgroup 2.3 the defect area became almost completely filled with new bones. Moreover, this new bone lamellae appeared irregularly organized with rough surface compared to smooth surfaced well organized original compact bone (Figure 5 F).

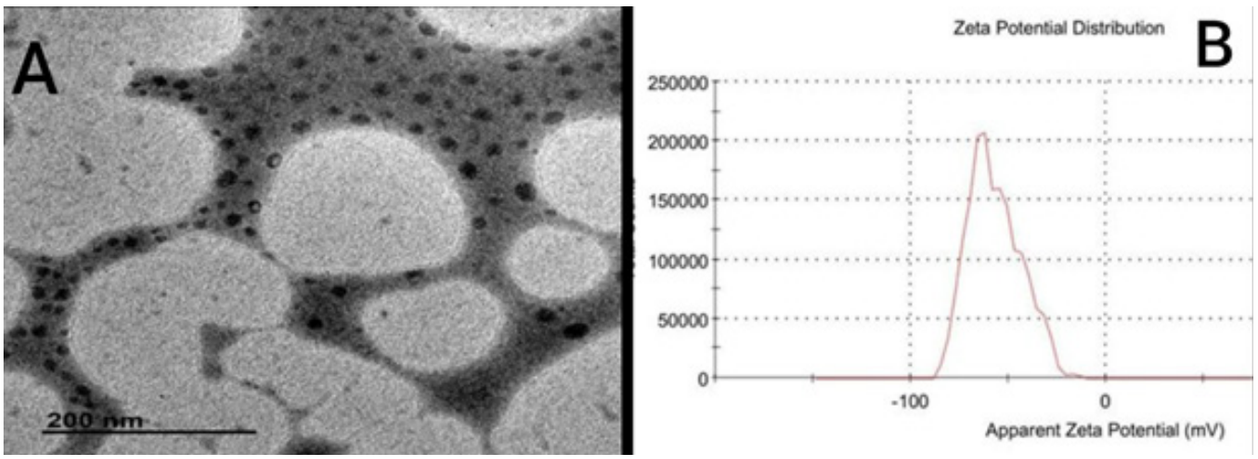


**Fig. 2:** The characterization of CTL-NE by TEM showing the spherical morphology of the nanoparticles with average size 460mm (A) and the zeta potential distribution of the nanoemulsion with average value - 60 mV (B).

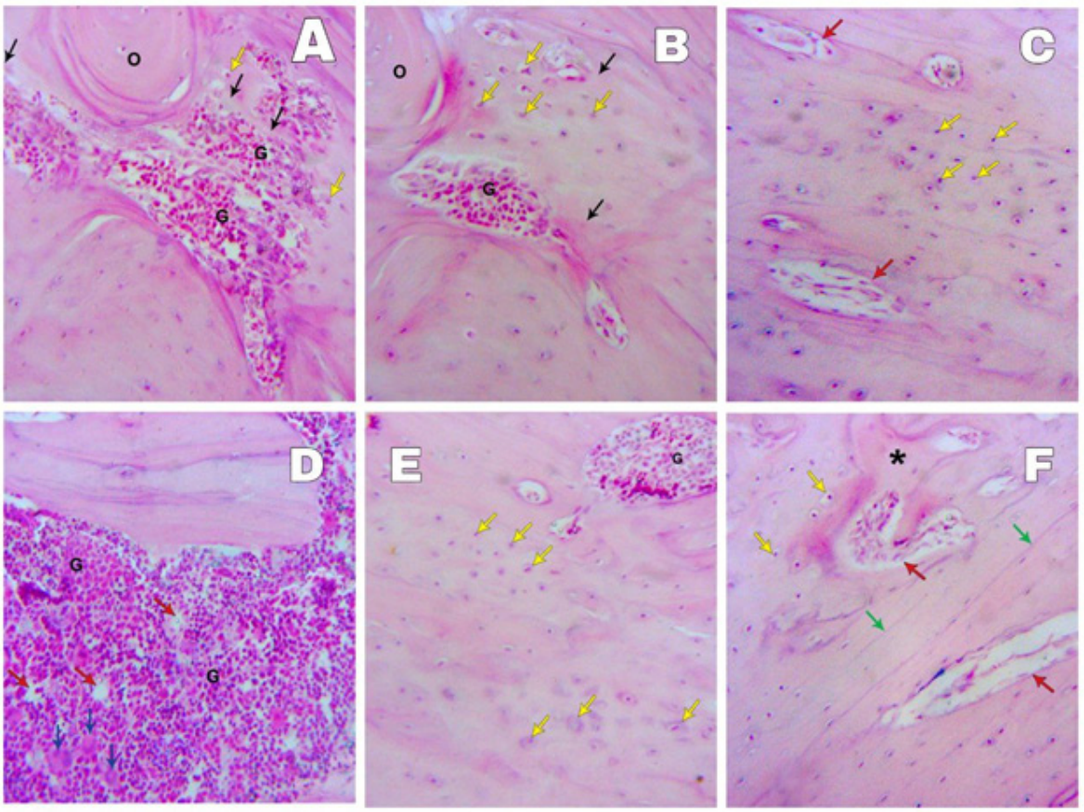


**Fig. 3:** Light micrographs of the mandibular bone defect in (A) subgroup 1.1 showing that the incompletely closed defect (black arrow) and the granulation tissue (G) filling part of the defect. (B) subgroup 1.2 reflecting the decrease in the defect size (G). (C) the defect site in subgroup 1.3 was almost completely healed. Note that few marrow spaces were still scattered within the bone (red arrow). (D) subgroup 2.1 defect site was almost filled with granulation tissue having numerous fat vacuoles (red arrow) and multinucleated giant cells (blue arrow). (E) subgroup 2.2 bony defect was incompletely closed by newly formed bone with enlarged osteocytes (yellow arrow) and the rest of the defect was still occupied by granulation tissue (G). (F) subgroup 2.3 defect site was almost completely closed with newly formed bone trabeculae. The marrow spaces (red arrow) were replaced by lamellar bone (*). Multiple dense resting lines were notable within the newly formed bone (green arrow). (H&E Orig. mag. X200)

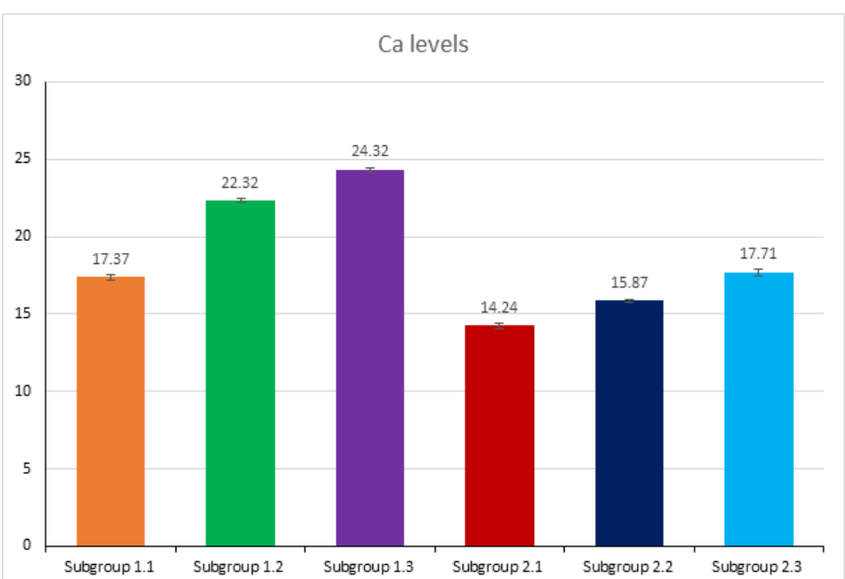


**Fig. 4:** Histogram showing statistical analysis of the quantity of Ca element in weight percentage existed in the bony defect of the studied subgroups. Data are presented as the mean ± standard deviation, *P value* ≤ 0.05.

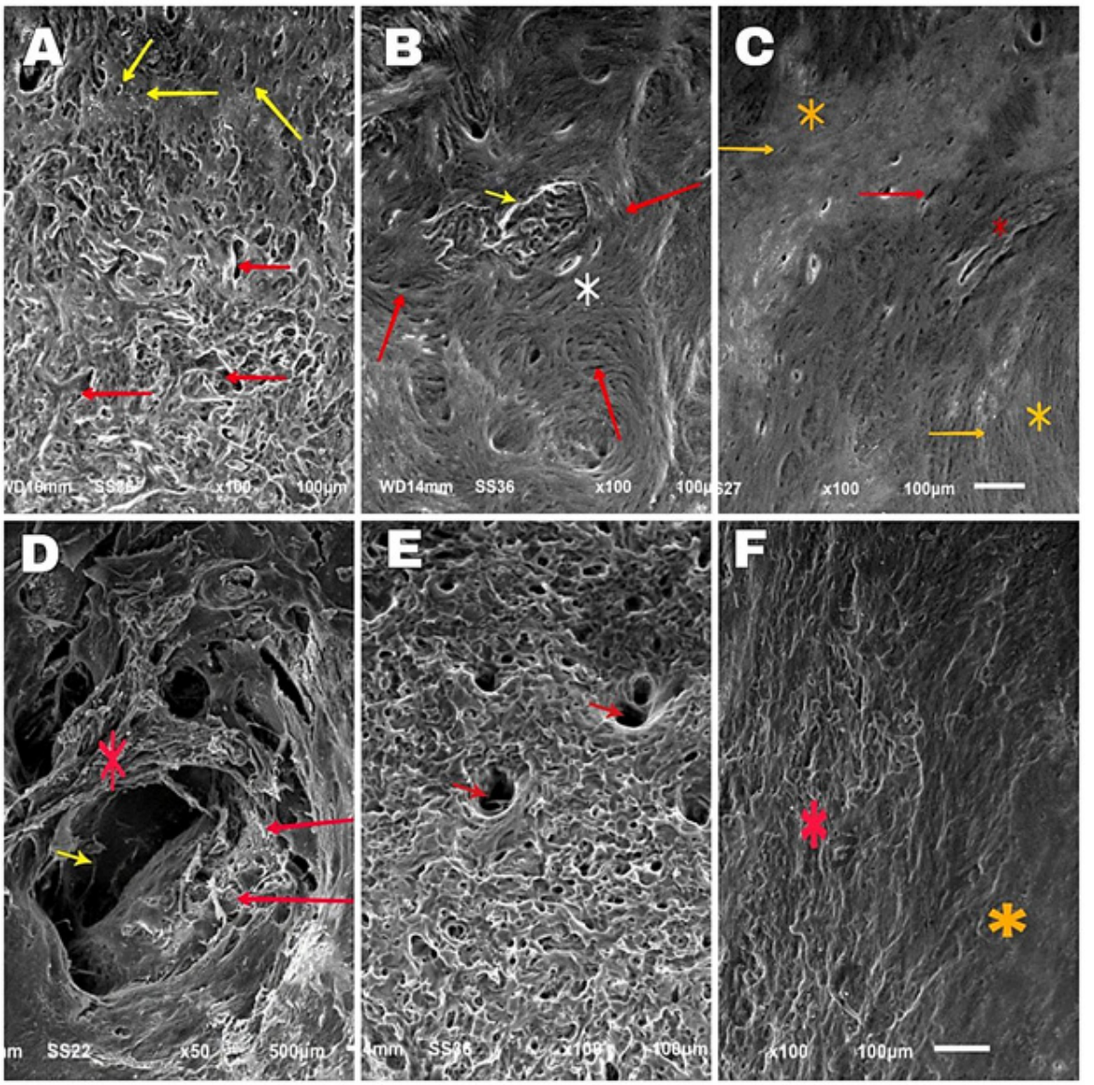


**Fig. 5:** Scanning electron micrograph of the mandibular bone defect in (A) subgroup 1.1 showing that it was almost filled with newly formed bone having disorganized trabeculae with numerous small marrow spaces (red arrow). (B) subgroup 1.2 healing callus had newly formed bone (yellow arrow) surrounded by lamellar bone (*) with elliptical shaped osteocytes lacunae (red arrow). In (C) subgroup 1.3 the defect was almost completely healed with callus lamellar bone (*) having less dense appearance compared with the original compact bone (*) and large elliptical osteocyte lacunae (red arrow) compared with the normal sized ones (yellow arrow). (D) subgroup 2.1 defect was filled with small bone callus (*). Scanty newly formed bone could be detected at the margins (red arrow). Note that large part of the defect appeared hollow and devoid of any healing callus (yellow arrow). (E) subgroup 2.2 showing that the healing callus was formed of unordered newly formed bone. Notice the widening of neurovascular openings (red arrow). (F) subgroup 2.3 showing that the bone plate regained its continuity with irregular callus lamellar bone (*) compared with the original smooth one (*)

## DISCUSSION

Our study's findings demonstrated the significant impact of OVX on bone healing and indicated that systemic delivery of CTL and CTL-NE may improve bone formation in mandibular bone defects in both OVX and sham rats, with CTL-NE having a preference.

The most widely used and established technique for creating an artificial PMOP in rats is the OVX rat model[14], and mandibular osteoporosis is thought to be a localized expression of this general osteoporosis in the oral and maxillofacial regions[15]. Furthermore, the jaw has been shown to have distinct tissue development origins and regeneration settings so we chose it to assess bone regenerative techniques using the mandibular bone defect model[16].

Both LM and SEM analyses were used in this qualitative study. While SEM showed the topographical characteristics of un-demineralized bone in bone defect locations, LM investigation used demineralized sections to illustrate the bone matrix architecture during bone healing. When compared to other subgroups, the qualitative analysis of subgroup 2.1 showed clear delays in osteogenesis and repair. These results were consistent with Tao *et al.*'s research from 2022, which found varying degrees of delayed bone repair in estrogen insufficiency conditions[17].

This defective bone healing may be attributed to estrogen deficiency related to dysregulation of bone cells activities. Several pathways and transcription factors essential in osteoblast differentiation are downregulated by estrogen deficiency, including WNT, TGFβ signaling pathway, BMP, and Runx2 causing decreased osteogenesis and adipogenic differentiation of mesenchymal stem cell to adipocytes, rather than osteoblast[18].

Moreover, hypoestrogenism promotes the differentiation and activation of osteoclasts by inducing the expression of RANKL and by downregulation of vascular endothelial growth factor (VEGF) and other angiogenic factors production impairing the angiogenesis[19]. Estrogen deficiency conditions also decrease osteocytes autophagy and increase their apoptosis. Furthermore, they promote osteocytes to produce RANKL and sclerotin with subsequent downregulation of Wnt signaling and reduction in bone formation[20].

According to other studies, the poor inflammatory response caused by inappropriate immune cells and inflammatory cytokine levels causes the delayed healing under estrogen deficient situations[21,22]. In the early and intermediate stages of OVX bone repair, Chen *et al*.[23] observed a decrease in M2 macrophage levels. Additionally, the expression of inflammatory cytokines, particularly TNF-α, was consistently up-regulated at other times and down-regulated during the onset of inflammatory reactions. Regretfully, Huang *et al*.[24] found that chronic TNF-α overexpression inhibited osteogenic development and caused oxidative damage. Furthermore, the multinucleated large cells that were present in the OVX defect area were discovered to be the osteoclast precursor cells, or "preosteoclast," and TNF-α enhances its sensitivity to RANKL through the AP-1 and NFκB signaling pathways, which promote osteoclast formation[25].

Delays in bone repair under estrogen-deficient conditions are intimately linked to the interactions between inflammation and oxidative stress, which have been thoroughly studied in several clinical scenarios[26]. This was also confirmed by Wu *et al*.[27] who reported diminished callus growth in OVX group with decreased mechanical properties compared with the sham one. They returned that to the impaired inflammatory response causing Nrf2 deficiency which in turn causes overproduction of ROS and deleterious oxidative stress.

Noteworthy in this study, quantitative X-ray elemental microanalysis of calcium level of the mandibular bony defect in OVX 2.1 subgroup illustrated a significant decrease below that of other subgroups. These results are comparable with those of Labah[28] and Atwa *et al*.[29] who reported a marked decrease in calcium content of the mandibular defects and femoral head epiphysis respectively in OVX groups. They attributed this deteriorated mineralization state to the abnormal bone turnover in which the rate of bone resorption outpaced the rate of bone synthesis.

Interestingly, CTL treated rats had better histological and ultrastructural bone healing results with a notable decrease in the defect size compared with those that didn't receive any treatment. These findings may be due to the anti-oxidation, anti-inflammation, neo-vascularization and immunomodulation activities of CTL[30]. These results coincided with those reported by Hu *et al*.[31] who proved that CTL promotes bone healing by upregulating osteogenic proteins (OPG and COL-1) and downregulating pre-inflammatory cytokines and chemokine.

Similarly, a study by Zeng *et al*.[32] reported that CTL exhibited immunomodulatory effects by controlling the signaling pathways of phosphatidylinositol 3-kinase/ protein kinase B (PI3K/AKT), T17 cell differentiation, MAPK, TNF, TGF-β/SMAD, IL-17, Janus kinase-signal transducers and activators of transcription (JAK-STAT), and other important signaling pathways by acting on important targets like TNF and IL6.

Xu Q. *et al*.[33] demonstrated that CTL reduced bone loss in the OVX-induced osteoporosis model by suppressing the NF-κB and MAPK signaling pathways mediated by Transforming Growth Factor β-activated kinase 1 (TAK1), which in turn inhibited osteoclast production and activity. Similarly, Li *et al*.[34] found that CTL could reduce bone loss and bone marrow adipose tissue (MAT) accumulation in both aged and OVX mice because it inhibits adipocyte differentiation in BMSCs by promoting osteoblast differentiation through the activation of the Adenosine monophosphate-activated protein kinase/ Sirtuin1-peroxisome gamma coactivator-1α (AMPK/ SIRT1-PGC-1α) signaling pathway, which is crucial for protecting against ROS accumulation in osteoporosis and skeletal aging by exerting antioxidant action.

Furthermore, our study's quantitative X-ray elemental microanalysis of the Ca level demonstrated that the defect region in CTL-treated mice had higher mineral content than their counterparts who received no treatment. Hu *et al*.[31] ascribed that to a markedly elevated carbonate content due to a slower bone turnover rate.

Both qualitative and quantitative evidence supported the current study's finding that CTL-NE-treated subgroups saw better bone repair. Similar outcomes were shown by Zhou *et al*.[35], who discovered that the therapeutic potential of CTL was enhanced following its incorporation into nanodrugs. Furthermore, they noticed that the half-life could be extended to 1 hour rather than just 24.6 minutes by the spherical nanoparticles that were created. Because of (i) increased drug solubility and oral bioavailability, (ii) longer blood circulation times due to improved protection before reaching the targeting sites, and (iii) targeted drug delivery to improve drug efficacy and reduce systemic toxicity, CTL nanoformulations improve therapeutic activities while offering a promising safety profile when compared to traditional formulations[36,37].

There are several restrictions on this study. First, we mainly examined CTL-NE's ability to regenerate bone

in the mandibular cortex; however, its effects on other types of bone remain to be investigated. Second, longer period studies to analyze the ability of CTL-NE to reach the absolute recovery of bone defects under estrogen deficiency conditions are highly recommended. Third, it is highly beneficial to study the anti-osteoporotic effect of CTL-NE on different bone tissue. Finally, it's extremely important to use CTL-NE in different dosages and to investigate its toxicity on different body tissues to find out the optimal therapeutic prescription.

## CONCLUSION

The beneficial effects of CTL in enhancing osteoporotic bone healing can be augmented by incorporating it into nanoemulsion formulations.

## ETHICS STATEMENT

The current study was carried out with approval number from the Suez Canal University Faculty of Dentistry's Research Ethics Committee (REC) (511/2022).

## CONFLICT OF INTERESTS

There are no conflicts of interest.

## REFERENCES


1. Geraci, A., Calvani, R., Ferri, E., Marzetti, E., Arosio, B., & Cesari, M. (2021). Sarcopenia and menopause: the role of estradiol. Frontiers in endocrinology, 12, 682012. DOI: 10.3389/fendo.2021.682012.
2. Song, S., Guo, Y., Yang, Y., & Fu, D. (2022). Advances in pathogenesis and therapeutic strategies for osteoporosis. Pharmacology & therapeutics, 237,108168. DOI: 10.1016/j.pharmthera.2022.108168.
3. Słupski, W., Jawień, P., & Nowak, B. (2021). Botanicals in postmenopausal osteoporosis. Nutrients, 13(5), 1609. DOI: 10.3390/nu13051609.
4. Shan, Y., Zhao, J., Wei, K., Jiang, P., Xu, L., Chang, C., …& He, D. (2023). A comprehensive review of Tripterygium wilfordii hook. f. in the treatment of rheumatic and autoimmune diseases: bioactive compounds, mechanisms of action, and future directions. Frontiers in Pharmacology, 14, 1282610. DOI.org/10.3389/fphar.2023.1282610
5. Shi, J., Li, J., Xu, Z., Chen, L., Luo, R., …& Zhang, C. (2020). Celastrol: A Review of Useful Strategies Overcoming its Limitation in Anticancer Application. Front. Pharmacol. 11, 11. DOI: 10.3389/fphar.2020.558741.
6. Wagh, P. R., Desai, P., Prabhu, S., & Wang, J. (2021). Nanotechnology-based celastrol formulations and their therapeutic applications. Frontiers in Pharmacology, 12, 673209. DOI.org/10.3389/fphar.2021.673209
7. Qiu, N., Liu, Y., Liu, Q., Chen, Y., Shen, L., Hu, M., …& Huang, L. (2021). Celastrol nanoemulsion induces immunogenicity and downregulates PD-L1 to boost abscopal effect in melanoma therapy. Biomaterials, 269,120604. DOI: 10.1016/j.biomaterials.2020.120604.
8. Charan, J., & Biswas, T. (2013). How to calculate sample size for different study designs in medical research?. Indian journal of psychological medicine, 35(2), 121-126. DOI: 10.4103/0253-7176.116232.
9. Ponnusamy, V., Solaiyappan, K., Govindarasu, M., Prathap, L., Babu, S. & Krishnan, M. (2023). Effect of estradiol on histopathology of brain in unilateral and bilateral ovariectomized rats. Bioinformation, 19(6),703. DOI: 10.6026/97320630019703.
10. Labah, D. A. (2023). Potential effect of platelet rich plasma as a promoter of bone healing in obese rats (histological and ultrastructural study). Egyptian Dental Journal, 69(1), 371-381. DOI: 10.21608/edj.2022.171428.2328.
11. Nie, Y., Fu, C., Zhang, H., Zhang, M., Xie, H., Tong, X., ... & Yan, M. (2020). Celastrol slows the progression of early diabetic nephropathy in rats via the PI3K/AKT pathway. BMC complementary medicine and therapies, 20, 1-14. DOI: 10.1186/s12906-020-03050-y.
12. Suckow, M., & Gimpel, J. (2020). Approaches to the humane euthanasia of research animals. Animal Biotechnology, 731. Academic Press. DOI:10.1016/B978-0-12-811710-1.00037-9.
13. Emara, R. S., & Noya, D. A. E. (2024). Comparative histological study on the possible protective effect of Mitoquinone versus Oxymatrine on cerebellar cortex of adult male albino rats treated with Sofosbuvir. Egyptian Journal of Histology. DOI: 10.21608/ejh.2024.252469.1979.
14. Yousefzadeh, N., Kashfi, K., Jeddi, S., & Ghasemi, A. (2020). Ovariectomized rat model of osteoporosis: a practical guide. EXCLI journal, 19, 89. DOI: 10.17179/excli2019-1990.
15. Jonasson, G., Skoglund, I., & Rythén, M. (2018). The rise and fall of the alveolar process: Dependency of teeth and metabolic aspects. Archives of oral biology, 96, 195-200. DOI: 10.1016/j.archoralbio.2018.09.016.
16. Liu, Z., Chen, R., Jiang, Y., Yang, Y., He, L., Luo, C., …. & Rong, L. (2019). A meta-analysis of serum osteocalcin level in postmenopausal osteoporotic women compared to controls. BMC musculoskeletal disorders, 20, 1. DOI: 10.1186/s12891-019-2863-y.
17. Tao, Z. S., Li, T. L., Xu, H. G., & Yang, M. (2022). Hydrogel contained valproic acid accelerates bone-defect repair via activating Notch signaling pathway in ovariectomized rats. Journal of Materials Science: Materials in Medicine, 33(1), 4. DOI: 10.1007/s10856-021-06627-2.

18. Khotib, J., Marhaeny, H. D., Miatmoko, A., Budiatin, A. S., Ardianto, C., Rahmadi, M., ... & Tahir, M. (2023). Differentiation of osteoblasts: the links between essential transcription factors. Journal of Biomolecular Structure and Dynamics, 41(19), 10257-10276. DOI: 10.1080/07391102.2022.2148749.

19. Eastell, R., O'Neill, T., Hofbauer, L., Langdahl, B., Reid, I., Gold, D. & Cummings, S. (2016). Postmenopausal osteoporosis'. Nature reviews Disease primers, 2(1), 1. DOI: 10.1038/nrdp.2016.69.

20. Florencio-Silva, R., Sasso, G. R., Sasso-Cerri, E., Simões, M. J., & Cerri, P. S. (2018). Effects of estrogen status in osteocyte autophagy and its relation to osteocyte viability in alveolar process of ovariectomized rats. Biomedicine & Pharmacotherapy, 98, 406-415. DOI: 10.1016/j.biopha.2017.12.089.

21. Ragipoglu, D., Hauff, K., Bülow, J., Voss, M., Haffner-Luntzer, M., Dudeck, A., … & Fischer, V. (2022). Mast cell deficiency improves compromised fracture healing after severe trauma. Bone Reports, 16, 01302. DOI: 10.3389/fimmu.2022.883707.

22. Haffner-Luntzer, M., Fischer, V., Prystaz, K., Liedert, A., & Ignatius, A. (2017). The inflammatory phase of fracture healing is influenced by oestrogen status in mice. European journal of medical research, 22, 1-11. DOI.org/10.1186/s40001-017-0264-y.

23. Chen, L., Cheng, S., Sun, K., Wang, J., Liu, X., Zhao, Y., ... & Shu, B. (2021). Changes in macrophage and inflammatory cytokine expressions during fracture healing in an ovariectomized mice model. BMC Musculoskeletal Disorders, 22(1), 494. DOI. org/10.1186/s12891-021-04360-z.

24. Huang, L., Lu, S., Bian, M., Wang, J., Yu, J., Ge, J., ... & Xu, Q. (2023). Punicalagin attenuates TNF-α-induced oxidative damage and promotes osteogenic differentiation of bone mesenchymal stem cells by activating the Nrf2/HO-1 pathway. Experimental Cell Research, 430(1), 113717. DOI.org/10.1016/j.yexcr.2023.113717.

25. Gambari, L., Grassi, F., Roseti, L., Grigolo, B., & Desando, G. (2020). Learning from monocyte-macrophage fusion and multinucleation: potential therapeutic targets for osteoporosis and rheumatoid arthritis. International Journal of Molecular Sciences, 21(17), 6001. DOI: 10.3390/ijms21176001.

26. Singh, V., & Ubaid, S. (2020). Role of silent information regulator 1 (SIRT1) in regulating oxidative stress and inflammation. Inflammation, 43, 1589-1598. DOI: 10.1007/s10753-020-01242-9.

27. Wu, X., Zhou, X., Liang, S., Zhu, X., & Dong, Z. (2021). The mechanism of pyrroloquinoline quinone influencing the fracture healing process of estrogen-deficient mice by inhibiting oxidative stress. Biomedicine & Pharmacotherapy, 139, 111598. DOI: 10.1016/j.biopha.2021.111598.

28. Labah, D. A. (2017). The validity of nano-chitosan/nano-hydroxyapatite as a promoter of bone healing in ovariectomized rats. Egyptian Dental Journal, 63(3-July (Oral Medicine, X-Ray, Oral Biology & Oral Pathology)), 2389-2402. DOI: 10.21608/edj.2017.76056.

29. Atwa, A., Mostafa, M. A., Song, S., & Sarhan, M. (2021). The Femoral Head Epiphysis of Ovariectomized Rats as A Site for Studies on Osteoporosis: Microstructural Changes Evaluations. Egyptian Academic Journal of Biological Sciences, D. Histology & Histochemistry, 13(1), 1-12. DOI: 10.21608/eajbsd.2021.145983

30. Xu, S., Feng, Y., He, W., Xu, W., Xu, W., Yang, H., & Li, X. (2021). Celastrol in metabolic diseases: Progress and application prospects. Pharmacological research, 167, 105572. DOI: 10.1016/j.phrs.2021.105572.

31. Hu, X., Gu, Y., Wu, Q., Jiang, F., & Song, Z. (2022). Celastrol enhances bone wound healing in rats. Acta Biochimica Polonica, 69(4), 839-845. DOI: 10.18388/abp.2020_6270.

32. Zeng, L., Yu, G., Yang, K., He, Q., Hao, W., Xiang, W., ... & Sun, L. (2024). Exploring the mechanism of Celastrol in the treatment of rheumatoid arthritis based on systems pharmacology and multi-omics. Scientific Reports, 14(1), 1604. DOI: 10.1038/s41598-023-48248-5. DOI: 10.1038/s41598-023-48248-5.

33. Xu, Q., Chen, G., Xu, H., Xia, G., Zhu, M., Zhan, H., ... & Liu, X. (2021). Celastrol attenuates RANKL-induced osteoclastogenesis in *vitro* and reduces titanium particle-induced osteolysis and ovariectomy-induced bone loss in *vivo*. Frontiers in Pharmacology, 12, 682541. DOI: 10.3389/fphar.2021.682541.

34. Li, L., Wang, B., Li, Y., Li, L., Dai, Y., Lv, G., ... & Li, P. (2020). Celastrol regulates bone marrow mesenchymal stem cell fate and bone-fat balance in osteoporosis and skeletal aging by inducing PGC-1α signaling. Aging (Albany NY), 12(17), 16887. DOI: 10.18632/aging.103590.

35. Zhou, M., Liao, J., Lai, W., Xu, R., Liu, W., Xie, D., ... & Li, G. (2023). A celastrol-based nanodrug with reduced hepatotoxicity for primary and metastatic cancer treatment. EBioMedicine, 94. DOI: 10.1016/j.ebiom.2023.104724.

36. Wagh, P. R., Desai, P., Prabhu, S., & Wang, J. (2021). Nanotechnology-based celastrol formulations and their therapeutic applications. Frontiers in Pharmacology, 12, 673209. DOI: 10.3389/fphar.2021.673209.

37. Li, C., Li, Y., Zeng, Q., Zhou, Y., Su, H., Han, Y., & Li, C. (2024). Celastrol nano-emulsions selectively regulate apoptosis of synovial macrophage for alleviating rheumatoid arthritis. Journal of Drug Targeting, 32(6), 724-735. DOI: 10.1080/1061186X.2024.2352757.

**الملخص العربى**

# التأثيرالمحتمل للسيلاسترول و جزيئاته النانونية على تجدد الجروح العظمية في الفئران المصابة بمرض هشاشة العظام الناتج عن ازالة المبايض

**ليلى فكرى الشاهد[١]، دعاء احمد لبح[١]، رشا محمود طه[٢]، تامر حسانين حسان[٣]، الهام محمود فتحى[٢]**

**قسم بيولوجيا الفم، كلية طب الاسنان، [١]جامعة الزقازق، [٢]جامعة قناة السويس**

**[٣]قسم الصيدلانيات كلية الصيدلة جامعة قناة السويس**

**المقدمة:** يعد مرض هشاشة العظام احد اهم الامراض التى تعقد التئام الجروح العظمية ويمكن أن يكون هذا مرتبطا بعوامل مختلفة. يمكن أن يساعد النظام الغذائي المحتوى على السلاستيرول او جزيئاته النانونية على اصلاح تلك العوامل خاصة تلك المرتبطة بإلجهاد التأكسدي وبالتالى تعزيز التئام تلك الجروح.

**الهدف من العمل:** دراسة تاثيرالسيلاسترول وجزيئاته النانونية على التئام الجروح العظمية فى الفئران المصابة بهشاشة العظام.

**منهجية البحث:** اجرى هذا البحث على ٦٠ من انثى الفئران مقسمةإلى مجموعتين رئيسيتين: المجموعة الأولى الخاضعة لعملية زائفة لاستئصال المبيضين وبعد ٦٠ يوما تم اجراء ازالة لجزء من عظم الفك سفلى لكل فأر, ثم تم تقسيم فئران هذه المجموعة بالتساوى الى ثلاث مجموعات فرعية وهى: المجموعة ١,١ التى لم يتم اعطاؤها أى أدوية ، والمجموعة ٢,١: تم اعطاؤها السيلاسترول ، و المجموعة ٣,١: تم اعطاؤها الجزيئات النانونية للسيلاسترول. المجموعة الثانية الخاضعة لاستئصال المبيضين وبعد ٦٠ يوما تم اجراء ازالة لجزء من عظم الفك سفلى, ثم تم تقسيم فئران هذه المجموعة ايضا الى ثلاث مجموعات فرعية وهى: المجموعة ١,٢: لم يتم اعطاؤها أى أدوية، والمجموعة ٢,٢: تم اعطاؤها السيلاسترول والمجموعة الفرعية ٣,٢: تم اعطاؤها الجزيئات النانونية للسيلاسترول. وفي نهاية التجربة التى استمرت ٤ اسابيع ، تم التضحية بالفئران وتحضير خمس عينات من الفكوك السفلية بكل مجموعة للفحص المجهري الضوئي وخمس عينات أخرى لتحليل العناصر بالأشعة السينية والمجهر الإلكتروني الماسح.

**النتائج:** أظهر الفحص النسيجي الدقيق تاخر الالتئام العظمى فى فئران المجموعة الثانية المصابة بهشاشة العظام كما أظهر التحليل الدقيق للعناصر بالجرح العظمى انخفاضًا كبيرًا في محتوى الكالسيوم مقارنة بفئران المجموعة الاولى. ومن المثير للاهتمام أن كلا المجموعتين حظت بتحسن ملحوظ فى الالتئام العظمى عند تناول الفئران السيلاسترول، على الرغم من ذلك فان افضل التئام للجرح العظمى يمكن ملاحظته فى المجموعات التى تم اعطاؤها الجزيئات النانونية للسيلاسترول . تم تأكيد هذه النتائج هستولوجيا ومن خلال التحليل الدقيق للعناصر الكالسيوم وباستخدام المجهر الإلكتروني الماسح.

**الخلاصة:** يمكن اعتبار الجزيئات النانونية للسيلاسترول علاجا فعالا لتعزيز التئام الجروح العظمية فى الفئران السليمة والمصابة بهشاشة العظام على حد سواء.